

Analysis of separation efficiency in capillary electrophoresis with direct control of electroosmosis by using an external electric field

CHENG S. LEE*, CHIN-TIAO WU, TERESA LOPES and BHISMA PATEL

Department of Chemical and Biochemical Engineering, University of Maryland Baltimore County Campus, Baltimore, MD 21228 (USA)

ABSTRACT

Direct control of electroosmosis in capillary electrophoresis with the application of an external electric field is demonstrated by the UV marker method. When the zeta potential at the capillary/aqueous solution interface is small, the capacitor model qualitatively and quantitatively predicts the effectiveness of the external electric field for controlling electroosmosis at different electrolyte concentrations and capillary dimensions. To investigate the separation efficiency of capillary electrophoresis with the direct control of electroosmosis, frontal analysis of dimethyl sulfoxide as a UV marker are examined. There is no measurable additional band broadening induced by the application of an external electric field.

INTRODUCTION

With the application of the current monitoring method [1], we have recently demonstrated the direct control of electroosmosis in capillary electrophoresis by using an additional electric field applied from outside the capillary [2,3]. This technique vectorally couples the externally applied electric potential with the internal electric potential across the buffer solution inside the capillary. This electric potential gradient across the capillary between the external and internal electric potential is uniform and constant along the length of the capillary. This newly created electric field is therefore perpendicular across the capillary and controls the polarity and magnitude of the zeta potential on the interior surface of the capillary wall. Because the direction and flow-rate of electroosmosis are dependent on the polarity and magnitude of the zeta potential [4], the electroosmotic flow can therefore be directly manipulated by simply varying the external electric potential.

To investigate the fundamentals of the use of an external electric potential for controlling the electroosmotic flow, a capacitor model as shown in Fig. 1 was proposed [3]. The capacitance of the electrostatic diffuse layer at the inner capillary/inner aqueous interface, C_{ei} in faraday at 25°C, was given by

$$C_{ei} = 228.5 \cdot 10^{-6} C^{1/2} \cosh(19.46 \zeta) \pi D_{id} l \quad (1)$$

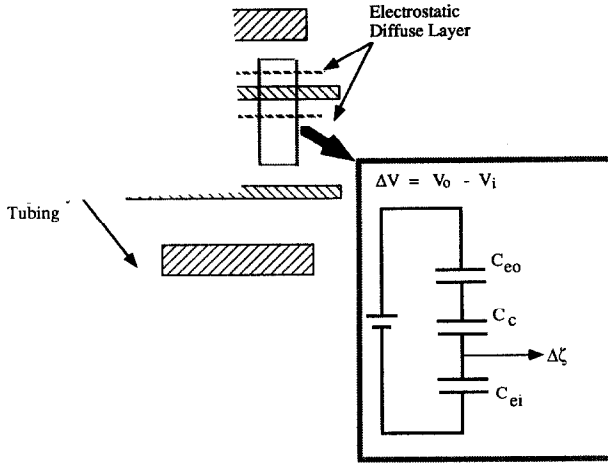


Fig. 1. The proposed capacitor model for predicting the change in the zeta potential due to the application of an external electric field.

where C is the concentration of ions in the solution in mol/l, ζ is the zeta potential at the capillary/aqueous interface in volts, D_{id} is the inner diameter of inner capillary tubing in cm and l is the length of capillary tubing in cm [4]. The capacitance of the inner capillary tubing, C_c , was given by

$$C_c = \varepsilon_c 2\pi l / [\ln(D_{od}/D_{id})] \quad (2)$$

where ε_c is the electrical permittivity of silica surface and D_{od} is the outer diameter of inner capillary tubing [5]. The capacitance of the electrostatic diffuse layer at the inner capillary/outer aqueous interface (in the annular space between the outer and inner capillaries), C_{eo} in faraday at 25°C, was given by

$$C_{eo} = 228.5 \cdot 10^{-6} C^{1/2} \cosh(19.46 \zeta) \pi D_{od} l \quad (3)$$

where D_{od} is the outer diameter of inner capillary tubing in cm [4]. The total capacitance of three capacitors in series, C_T , was given as [5]

$$(C_T)^{-1} = (C_{eo})^{-1} + (C_c)^{-1} + (C_{ei})^{-1} \quad (4)$$

Because the capacitance of the electrostatic layer was much greater than that of the capillary tubing for the accumulation of mobile ions in the electrostatic layer, the total capacitance, C_T , was simplified to

$$C_T = C_c \quad (5)$$

The change in the zeta potential at the inner capillary/inner aqueous interface, $\Delta \zeta$, due to the applied potential gradient across the inner capillary wall, ΔV , was given by [5]

$$\Delta\zeta = \Delta V/[(C_{ei})/(C_T)] = \Delta V/[(C_{ei})/(C_c)] \quad (6)$$

The change in the zeta potential was then converted to the change in the electroosmotic mobility for the comparison with the experimental results [3].

Direct control of electroosmosis with the application of an external electric field under various operating conditions including different solution pHs, electrolyte concentrations and capillary dimensions were examined [3]. The experimental results were then compared with the predictions obtained from the capacitor model. In a previous study [3], the capacitor model only predicted the trend of experimental results at various operating conditions, and failed as a quantitative model for predicting the effectiveness of the applied external electric field for controlling the electroosmotic flow.

One problem was encountered in the comparison of experimental results with the predictions from the capacitor model. Owing to the nature of the current monitoring method employed in the experiment for measuring the change in the electroosmotic flow [2,3], the electrolyte concentration inside the inner capillary tubing was varied during the measurement. Thus, an average electrolyte concentration was used for the calculation of the capacitance of the electrostatic diffuse layer as shown in eqn. 1 in the capacitor model. The use of an average electrolyte concentration in the calculation may affect the ability of the capacitor model to predict the experimental results quantitatively. To examine this issue, the UV marker method [6] was used in this study for measuring the changes in the direction and rate of the electroosmotic flow on application of an external electric field. In contrast to the current monitoring method, the electrolyte concentration in the capillary tubing was kept constant during the experiment with the use of UV marker method. Further, frontal analyses of the UV marker were examined for investigating the separation efficiency of capillary electrophoresis with the direct control of electroosmosis.

EXPERIMENTAL

A complete capillary electrophoresis system with a UV detector as shown in Fig. 2 was installed in our laboratory for delivering electric fields both externally through the annulus between the inner and outer capillaries and internally across the buffer solution in the inner capillary. A 23-cm fused-silica capillary with 25 μm I.D. (150 μm O.D.) or 50 μm I.D. (150 μm O.D.) was placed inside a larger capillary (250 μm I.D., 375 μm O.D.) which was 20 cm long. The smaller (inner) capillary was attached between reservoirs 1 and 4 while the larger (outer) capillary was attached between reservoirs 2 and 3. The inner capillary tubing without the external polyimide coating was obtained from Polymicro Technologies (Phoenix, AZ, USA). A 1-mm section of the polyimide coating on the exterior surface of the outer capillary tubing was removed by using concentrated sulfuric acid solution to create a window for the UV radiation.

Two high-voltage power supplies were obtained from Spellman High-Voltage Electronics (Plainview, NY, USA). One high-voltage power supply was connected to reservoirs 2 and 3 so that an outer electric field was applied to the annular space between the two capillaries. The annular space was filled with a 1 mM phosphate buffer solution (pH 6) as the conductive medium for applying the outer electric field.

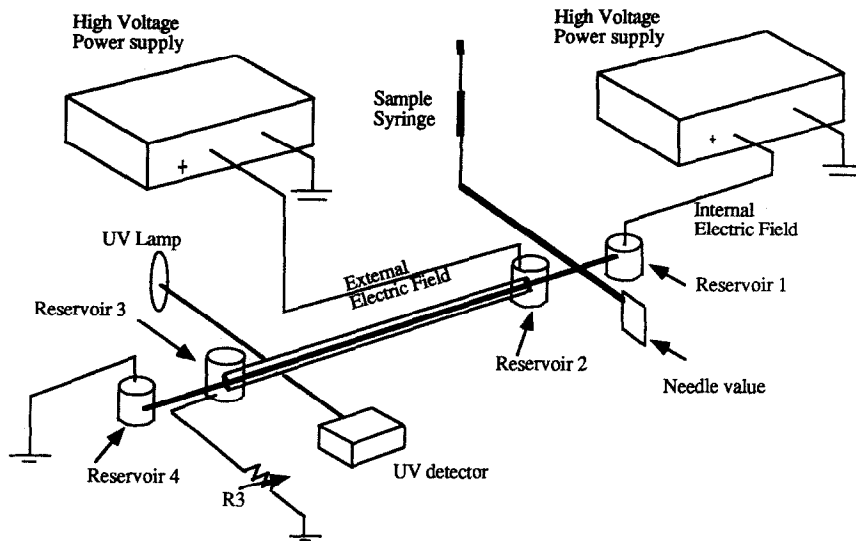


Fig. 2. A complete capillary electrophoresis system with a UV detector delivers the electric fields both externally through the annulus between the inner and outer capillaries and internally across the buffer solution in the inner capillary.

A circulation pump was used to accelerate a fluid flow in the annulus between the inner and outer capillaries. This fluid flow was to enhance the heat transfer in the annulus for removing the additional heat generated by the application of external electric field. Another high-voltage power supply connecting reservoir 1 with reservoir 4 applied a constant inner electric potential of 5.5 kV inside the inner capillary. The inner electric field strength was therefore equal to $5.5 \text{ kV}/23 \text{ cm} = 239 \text{ V/cm}$. With adjustable resistor R3, we were able to establish a constant electric potential gradient between the inner and outer electric potential along the 20-cm long annulus between reservoirs 2 and 3. This newly created electric field was perpendicular across the wall of the inner capillary and controlled the zeta potential at the inner capillary/inner aqueous interface. By varying the outer electric field and the resistance of R3, various electric fields (potential gradients) across the inner capillary were generated.

A UV detector from Linear Instruments (Reno, NV, USA) was used for monitoring the change in the direction and rate of the electroosmotic flow on application of an external electric field in the UV marker method [6]. The distance between reservoir 1 and the UV detector was 14.5 cm. An uncharged marker solute (no electrophoretic mobility) such as dimethyl sulfoxide with UV absorbance was selected for this study. Dimethyl sulfoxide was carried through the capillary under the action of only the electroosmotic flow inside the capillary. The changes in the elution time of the front of a 0.1% dimethyl sulfoxide solution from reservoir 1 to the UV detector were recorded as the externally electric field was changed. With this set-up and procedure, we were able to monitor the direction and rate of electroosmotic flow with or without an additional external electric field during the experiment. In addition, the number of theoretical plates, N , with the direct control of electroosmosis was measured from the shape of the front [7].

Sodium phosphate buffer, dimethyl sulfoxide and hydrochloric acid were purchased from Sigma (St. Louis, MO, USA). The pH of the buffer solution was adjusted with 0.1 M hydrochloric acid.

RESULTS AND DISCUSSION

The experimental results for the control of electroosmosis inside a 50 μm I.D. \times 150 μm O.D. inner capillary tubing with 1 mM phosphate buffer (pH 6) were used for comparisons with the predictions obtained from the capacitor model. Details of the calculation of the capacitor model were discussed previously [3]. As shown in Fig. 3, the capacitor mode still failed to predict quantitatively the observed changes in the electroosmotic mobility even with the application of the UV marker method. The positive value of the electroosmotic mobility indicated that the direction of flow was from reservoir 1 to reservoir 4 when the cathode end of inner electric field was at reservoir 4. The experimental error in measuring the change in the electroosmotic flow was about 1–3% for various potential gradients for over five runs.

The zeta potential at the aqueous/inner capillary interface was calculated by using the measured electroosmotic mobility [4]. The zeta potential in the presence of a zero potential gradient (between the outer and inner electric potential) was decreased from -49 to -4 mV by changing the solution conditions from a 1 mM phosphate buffer of pH 6 to a 10 mM phosphate buffer of pH 2.7. The decrease in the zeta potential was due to the application of a higher ionic strength and a lower pH at the inner capillary/inner aqueous interface [4]. As shown in eqn. 1, the capacitance of the electrostatic diffuse layer decreased with decrease in the zeta potential. However, the use of a higher buffer concentration (10 mM) increased the capacitance of the electrostatic diffuse layer. The effect of the buffer concentration was greater than the effect of the zeta potential on the capacitance of the electrostatic diffuse layer, as shown in eqn. 1. Thus, the capacitance of the electrostatic diffuse layer was greater with 10 mM phosphate buffer of pH 2.7 than with 1 mM phosphate buffer of pH 6. As shown in

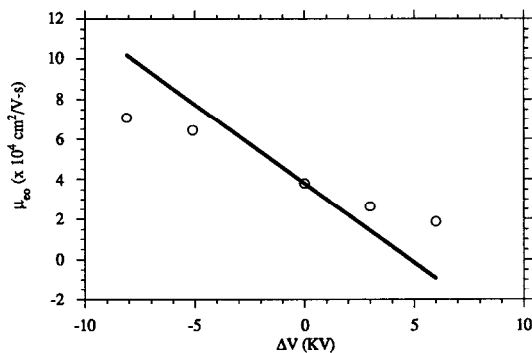


Fig. 3. Plot of electroosmotic mobility, μ_{eo} , against applied potential gradient, ΔV . (○) Experimental data for 1 mM phosphate buffer (pH 6) with the use of a 50 μm I.D. \times 150 μm O.D. inner capillary tubing in the UV marker method. Solid line, predictions obtained from the capacitor theory. The positive value of electroosmotic mobility indicates that the direction of flow is from reservoir 1 to reservoir 4 when the cathode end of inner electric field is at reservoir 4.

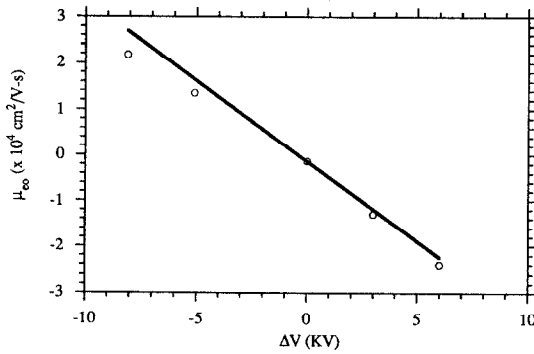


Fig. 4. Plot of electroosmotic mobility, μ_{∞} , against applied potential gradient, ΔV . Details as in Fig. 3 except that 10 mM phosphate buffer (pH 2.7) was used.

eqn. 6, the larger capacitance of the electrostatic diffuse layer in the solution of 10 mM phosphate buffer at pH 2.7 would result in less control of the electroosmotic flow. This theoretical analysis qualitatively explained why the range of controlled electroosmotic mobility as shown in Fig. 4, between $-2 \cdot 10^{-4}$ and $+2 \cdot 10^{-4}$ cm²/V·s, was less than that as shown in Fig. 3, between $+7 \cdot 10^{-4}$ and $+2 \cdot 10^{-4}$ cm²/V·s. Further, the capacitor model quantitatively predicted the observed changes in the electroosmotic mobility with the application of various potential gradients as shown in Fig. 4. The experimental error in measuring the change in the electroosmotic flow was about 1% for various potential gradients for over five runs. The only significant difference in the solution conditions between the previous study [3] and the experimental results shown in Fig. 4 was the solution pH. At solution pH 2.7, the zeta potential in the presence of a zero potential gradient was -4 mV, close to zero. Was this the reason for achieving relatively good agreement between the experimental results shown in Fig. 4 and the predictions from the capacitor model? To answer this question, the direct control of electroosmosis inside a $25 \mu\text{m}$ I.D. \times $150 \mu\text{m}$ O.D. inner capillary was investigated under solution conditions of pH 2.7 with 1 and 10 mM phosphate buffers.

The experimental results for the control of electroosmosis inside a $25 \mu\text{m}$ I.D.

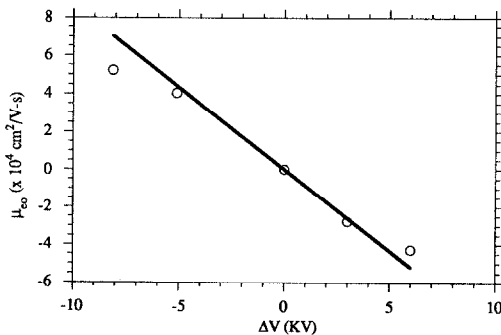


Fig. 5. Plot of electroosmotic mobility, μ_{∞} , against applied potential gradient, ΔV . Details as in Fig. 3 except that the buffer pH was 2.7 and $25 \mu\text{m}$ I.D. \times $150 \mu\text{m}$ O.D. inner capillary tubing was used.

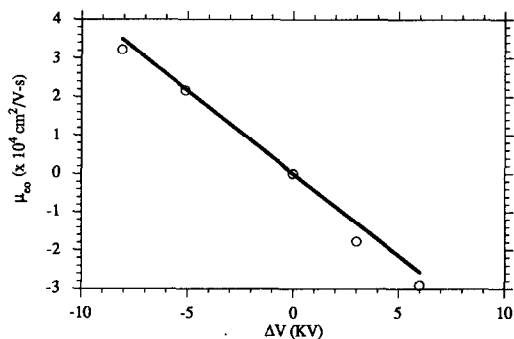


Fig. 6. Plot of electroosmotic mobility, μ_{eo} , against applied potential gradient, ΔV . Details as in Fig. 5. except that the phosphate buffer concentration was 10 mM.

$\times 150 \mu\text{m}$ O.D. inner capillary tubing at pH 2.7 with 1 and 10 mM phosphate buffer were used to compare with the predictions obtained from the capacitor model. As shown in Figs. 5 and 6, the capacitor model quantitatively predicted the effectiveness of the applied potential gradient for controlling the electroosmotic flow. The experimental error in measuring the change in the electroosmotic flow was about 1% for various potential gradients for over five runs. The experimental results shown in Figs. 5 and 6 further supported the proposed hypothesis: the use of a lower solution pH for obtaining a smaller zeta potential was essential for achieving relatively good agreement between the experimental results and the predictions from the capacitor model. This conclusion is currently used in efforts to improve the capacitor model as a quantitative model for predicting the effectiveness of the applied external electric field in the direct control of electroosmosis.

The external electric field was applied to the 20-cm long annular space between the inner and outer capillaries filled with the phosphate buffer solution. Only 20 cm of the 23-cm long inner capillary tubing was affected by the external electric field for controlling the electroosmotic flow inside the inner capillary. In this current configuration, the flow disturbance and mixing at the interface between the controlled and

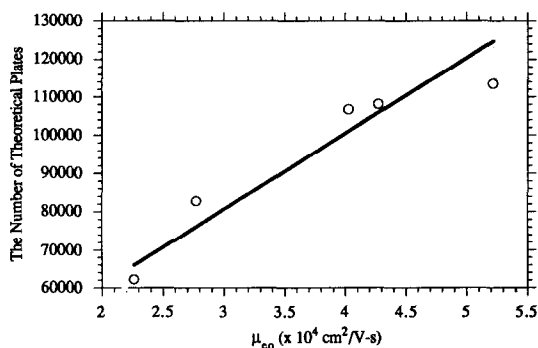


Fig. 7. Plot of number of theoretical plates against the absolute value of the electroosmotic mobility, μ_{eo} , measured from the experiment. (O) Number of theoretical plates measured with 1 mM phosphate buffer (pH 2.7) with the use of a $25 \mu\text{m}$ I.D. $\times 150 \mu\text{m}$ O.D. inner capillary tubing. Solid line, number of theoretical plates calculated from the molecular diffusion.

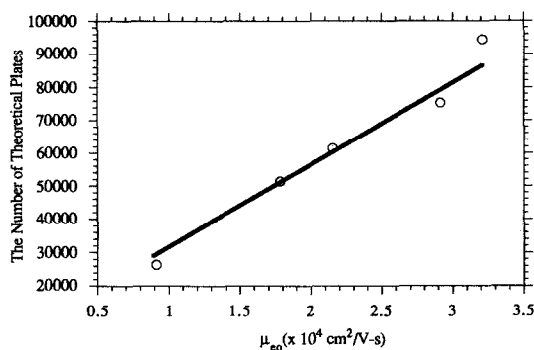


Fig. 8. Plot of number of theoretical plates against the absolute value of the electroosmotic mobility, μ_{eo} , measured from the experiment. Details as in Fig. 7 except that the phosphate buffer concentration was 10 mM.

uncontrolled regions in the inner capillary could possibly cause the additional dispersion and band broadening. To investigate this potential problem, frontal analyses of a 0.1% dimethyl sulfoxide in a $25 \mu\text{m}$ I.D. \times $150 \mu\text{m}$ O.D. inner capillary tubing at pH 2.7 with 1 and 10 mM phosphate buffer solutions were studied. As shown in Figs. 7 and 8, the number of theoretical plates measured from the experiment was plotted against the absolute value of the corresponding electroosmotic mobility measured from the experiment. The experimental error in measuring the number of theoretical plates was about 5–10% for various electroosmotic mobilities for over five runs. By assuming that molecular diffusion alone was responsible for zone broadening, the number of theoretical plates was also calculated [8]. A value of $5 \times 10^{-6} \text{ cm}^2/\text{s}$ was used as the diffusion coefficient of dimethyl sulfoxide in the calculation. The number of theoretical plates obtained from the calculation was then compared with the number of theoretical plates measured from the experiment. As shown in Figs. 7 and 8, the comparisons clearly indicated that there was no measurable additional dispersion and band broadening induced by the direct control of electroosmosis.

ACKNOWLEDGEMENTS

Support for this work by Engineering Research Center of the University of Maryland and Petroleum Research Grant administered by the American Chemical Society is gratefully acknowledged.

REFERENCES

- 1 X. Huang, M. J. Gordon and R. N. Zare, *Anal. Chem.*, 60 (1988) 1837.
- 2 C. S. Lee, W. C. Blanchard and C. T. Wu, *Anal. Chem.*, 62 (1990) 1550.
- 3 C. S. Lee, D. McManigill, C. T. Wu and B. Patel, *Anal. Chem.*, 63 (1991) 1519.
- 4 R. J. Hunter, *Zeta Potential in Colloid Science: Principles and Applications*, Academic Press, New York, 1981.
- 5 F. W. Sears, H. D. Zemasky and H. D. Young, *University Physics*, Addison-Wesley, Readings, MA, 1979.
- 6 T. Tsuda, K. Nomura and G. Nakagawa, *J. Chromatogr.*, 248 (1982) 241.
- 7 D. McManigill, personal communication, 1990.
- 8 J. W. Jorgenson and K. D. Lukacs, *Anal. Chem.*, 53 (1981) 1298.